Electronic Supplementary Material (ESI) for ChemComm.

Reversible 1D chain-reaction gives rise to an atomic-scale Newton's cradle

Lydie Leung‡, Matthew J. Timm‡ and John C. Polanyi*

Lash Miller Chemical Laboratories, Department of Chemistry, University of Toronto,

80 St. George Street, Toronto, ON M5S 3H6, Canada

‡ These authors contributed equally to the work

*Corresponding author: John C. Polanyi (john.polanyi@utoronto.ca).

Experimental Methods

All experimental work was conducted in an ultra-high vacuum (UHV) system composed of a low temperature scanning tunneling microscope (LT-STM) chamber (Omicron Nanotechnology; base pressure $< 1 \times 10^{-11}$ mbar) attached to a preparation chamber (base pressure $< 3 \times 10^{-11}$ mbar). All imaging was recorded at 4.6 K. Typical imaging conditions involved sample biases between -50 and 50 mV and tunneling currents < 1.0 nA, in the constant current mode. The Cu(110) crystal were cleaned by repeated cycles of argon ion bombardment (~7 μA drain current, 0.6 keV beam energy) and annealed to ~800 K by electron bombardment. The Cu surface cleanliness was assessed by STM. Trifluoroiodomethane (CF_3I; Synquest, purity: 99%) was deposited via a capillary tube onto the Cu surface at 77.8 K. After deposition, chemisorbed CF_3 and I atoms as well as lines of CF_3 molecules were observed on the surface. The tungsten STM tip was functionalized by repeated -5 to -10 V pulses over CF_3 and I-atom clusters, until the apparent height of a CF_3 molecule was measured as 3× greater than that obtained from a non-functionalised tip. Electron-induced dissociation of chemisorbed CF_3 molecules was performed by (i) locating the tip over it, (ii) adjusting the tip height and (iii) ramping the sample bias to V_{pulse} (1.3 - 1.8 V) with the feedback loop turned off. Dissociation was confirmed in a subsequent scanning image. STM images were analysed using the WSxM Software.[1] The terminal CF_2 was produced by the electron-induced dissociation of a terminal CF_3 molecule of a line of CF_3 (Fig.1 and 3).

Adsorption Calculation Methods

Density function theory (DFT) calculations were performed using the Vienna *Ab initio* Simulation Package (VASP)[2,3] to obtain the adsorption geometries matching whose obtained by STM. The projector augmented wave (PAW) method[4,5] and the generalized gradient approximation (GGA) with the Perdew-Burke-Ernzerhof (PBE) functional[6] were used for the calculations. Van der Waals interactions were corrected by the addition of Grimme's semi-empirical dispersion correction (DFT-D3).[7] The energy cutoff for the plane-wave basis set was 400 eV. All calculations were computed on the SciNet supercomputer Niagara cluster.[8,9]

The Cu(110) surface was modeled as a (3 × 14) supercell composed of 210 Cu-atoms arranged in five layers and separated by a 17 Å vacuum region. All atoms were allowed to move except for the last two layers, which were frozen at the theoretically optimized Cu lattice constant of 3.5673 Å. The adsorption geometries were calculated by relaxing the adsorbate plus Cu-slab system until the force on each relaxed atom was < 0.01 eV/Å. The calculations were performed using single Γ-point *k*-mesh sampling. The adsorption geometries are depicted below the STM images in Fig.1 and 3, and are labelled 'TH' to denote the 'Theory' used.

Climbing Image Nudged Elastic Band Calculation Methods

The nudged elastic band (NEB) and climbing image nudged elastic band (CI-NEB) calculations[10,11] were performed in VASP, under the same conditions as the adsorption geometry calculations. Prior to conducting the CI-NEB calculations, NEB calculations were performed for each molecular line to identify the local minima and maxima along the minimum energy pathway between the initial and final states (IS and FS). The NEB and CI-NEB calculations were optimized until the forces orthogonal to the nudged elastic band were < 0.02 eV/ Å. The Fast Inertial Relaxation Engine (FIRE) optimizer[12] was used to minimize the

forces. The IS and FS for the NEB and CI-NEB calculations were taken from the adsorption geometries calculated for Fig. 1a, 1b and 1c.

For the bi-molecular line (Fig. 2a), a NEB calculation was performed using nineteen interstitial images between the IS and FS. A CI-NEB calculation with the same number of images was perfomed to obtain the barrier to reaction.

For the tri-molecular line (Fig. 2b), a NEB calculation was performed using twenty-two interstitial images between the IS and FS. In this calculation a local minimum was found along the reaction coordinate between the IS and FS states (corresponding to CI-NEB image 8, Fig. 2b), following dissociation of the in-plane C-F bond of the CF_3 precursor. This minimum was relaxed following the same procedure as that described for the relaxation of the IS and FS states. For the CI-NEB calculation, seven interstitial images were used to obtain the barrier between the IS and this local minimum. To obtain the barrier (the TS) between the local minimum and the FS, fifteen interstitial images were used. This is the barrier for a single knock-on reaction.

For the quadri-molecular line (Fig. 2c), a NEB was performed using thirty-two interstitial images between the IS and FS. In this calculation three local minima were found along the reaction coordinate between the IS and FS. The first local minimum (corresponding to image 6, Fig. 2c) followed dissociation of the in-plane C-F bond of the CF_3 precursor, the second local minimum (corresponding to image 18, Fig. 2c) followed the first knock-on, and the third local minimum (corresponding to image 30, Fig. 2c) followed the second knock-on. These minima were relaxed by the same procedure as described for the relaxation of the IS and FS. The CI-NEB calculation used five interstitial images to obtain the barrier between the IS and the first local minimum. To obtain the barrier corresponding to F—CF_2—F′, between the first local minimum and the second, eleven interstitial images were used. To obtain the barrier corresponding to F′—CF_2—F″, between the second local minimum and the third, eleven interstitial images were used. The barrier between the third local minimum and the FS was obtained using five interstitial images.

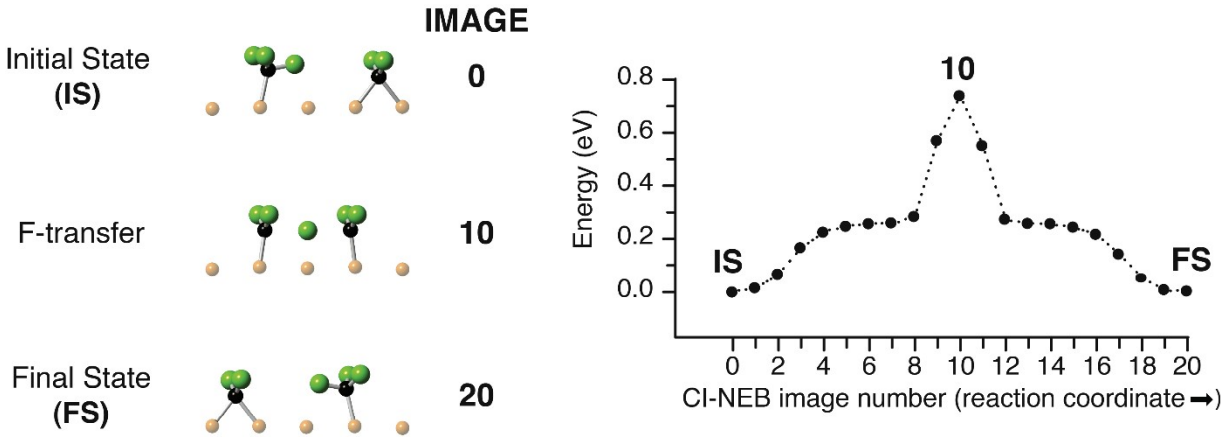

Figure S1 Climbing image-nudged elastic band (CI-NEB) pathway for F-atom transfer in the bi-molecular line. Minimum-energy pathway across a DFT potential energy surface as obtained from a CI-NEB calculation. Three representative CI-NEB images along the pathway are shown at the left of the figure.

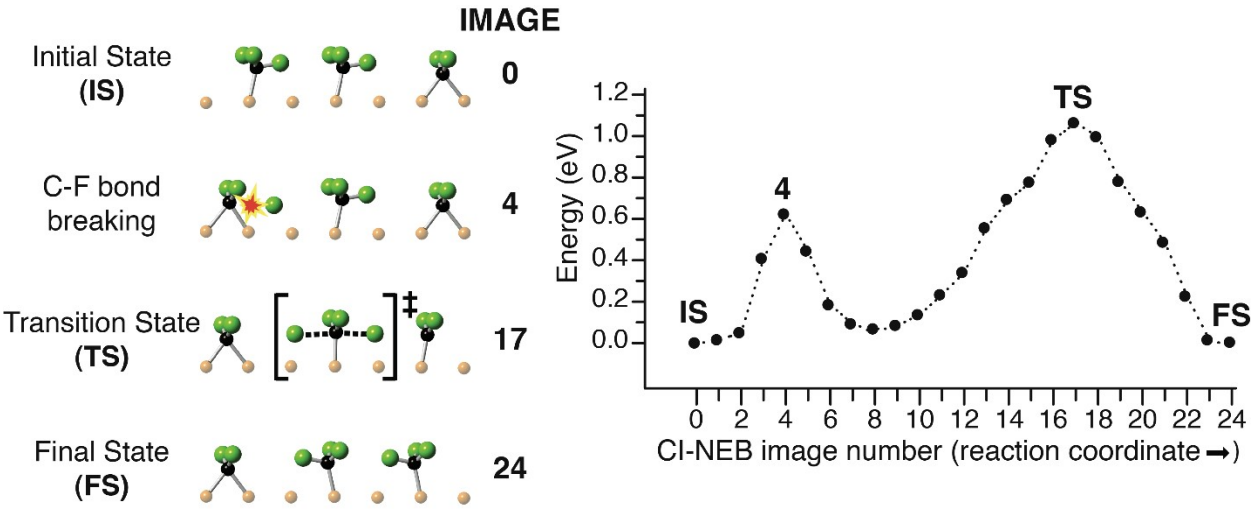

Figure S2 Climbing image-nudged elastic band (CI-NEB) pathway for the one knock-on reaction in the tri-molecular line. Minimum-energy pathway across a DFT potential energy surface as obtained from a CI-NEB calculation. Four representative CI-NEB images along the pathway are shown at the left of the figure.

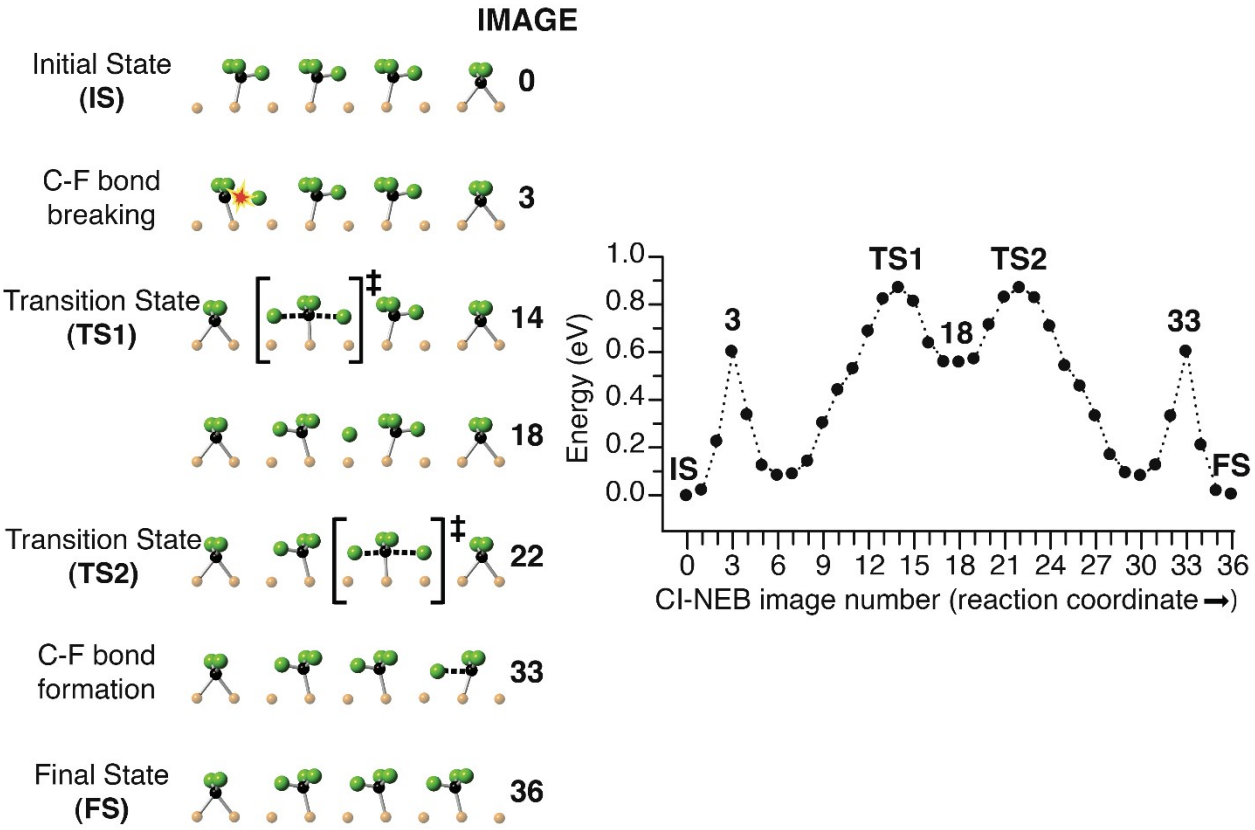

Figure S3 Climbing image-nudged elastic band (CI-NEB) pathway for the two knock-on reaction in the quadri-molecular line. Minimum-energy pathway across a DFT potential energy surface as obtained from a CI-NEB calculation. Seven representative CI-NEB images along the pathway are shown at the left of the figure.

Table S1: Ratio of the measured slopes S1:S2 (absolute values) for the chemisorbed CF_3 molecules (reading from left to right) in the quadri-molecular line shown in Figure 3.

Figure	For first CF_3 (Å/Å)	For second CF_3 (Å/Å)	For third CF_3 (Å/Å)
3a' S1 < S2	|0.150±0.004| **:** |0.194±0.004|	|0.168±0.003| **:** |0.197±0.003|	|0.124±0.003| **:** |0.129±0.003|
3b' S1 > S2	|0.284±0.011| **:** |0.160±0.002|	|0.209±0.004| **:** |0.142±0.002|	|0.191±0.004| **:** |0.163±0.003|
3c' S1 < S2	|0.156±0.004| **:** |0.196±0.003|	|0.159±0.004| **:** |0.194±0.005|	|0.132±0.003| **:** |0.151±0.003|
3d' S1 >S2	|0.259±0.010| **:** |0.162±0.003|	|0.211±0.004| **:** |0.145±0.004|	|0.232±0.005| **:** |0.168±0.003|
3e' S1 < S2	|0.163±0.004| **:** |0.196±0.003|	|0.155±0.005| **:** |0.175±0.004|	|0.124±0.003| **:** |0.142±0.006|
3f' S1 > S2	|0.278±0.010| **:** |0.156±0.003|	|0.224±0.006| **:** |0.156±0.002|	|0.219±0.005| **:** |0.145±0.003|
3g' S1 < S2	|0.159±0.005| **:** |0.178±0.005|	|0.152±0.004| **:** |0.183±0.005|	|0.116±0.003| **:** |0.137±0.007|

Supplementary Movie S1

Visualisation of the observed transfer of an F-atom from left to right along a line of fluorocarbon adsorbates on Cu(110), and subsequently for the reverse transfer from right to left. Below is a movie of the motion of a macroscopic Newton's cradle, synchronized with the atomic motion.

References

1. I. Horcas, F. Fernández, J. M. Gómez-Rodríguez, J. Colchero, J. Gómez-Herrero and A. M Baro, *Rev. Sci. Instrum.*, 2007, **78**, 013705.
2. G. Kresse and J. Hafner, *Phys. Rev. B*, 1993, **47**, 558–561.
3. G. Kresse and J. Furthmüller, *Phys. Rev. B*, 1996, **54**, 11169–11186.
4. P. E. Blöchl, *Phys. Rev. B*, 1994, **50**, 17953– 17979.
5. G. Kresse and D. Joubert, *Phys. Rev. B*, 1999, **59**, 1758– 1775.
6. J. P. Perdew, K. Burke and M. Ernzerhof, *Phys. Rev. Lett*., 1996, **77**, 3865– 3868.
7. S. Grimme, J. Antony, S. Ehrlich and H. Krieg, *J. Chem. Phys.*, 2010, **132**, 154104.
8. C. Loken, D. Gruner, L. Groer, R. Peltier, N. Bunn, M. Craig, T. Henriques, J. Dempsey, C.-H. Yu, J. Chen, L. J. Dursi, J. Chong, S. Northrup, J. Pinto, N. Knecht and R. Van Zon, *J. Phys.: Conf. Ser.*, 2010, **256**, 012026.
9. M. Ponce, R. van Zon, S. Northrup, D. Gruner, J. Chen, F. Ertinaz, A. Fedoseev, L. Groer, F. Mao, B. C. Mundim, M. Nolta, J. Pinto, M. Saldarriaga, V. Slavnic, E. Spence, C.-H. Yu and W. R. Peltier, *Practice and Experience in Advanced Research Computing* (PEARC'19), Chicago, IL, USA ACM, New York, NY, USA, 2019, **34**, 1–8.

10. G. Henkelman, B. P. Uberuaga and H. Jónsson, *J. Chem. Phys.*, 2000, **113**, 9901– 9904.
11. G. Henkelman and H. Jónsson, *J. Chem. Phys.*, 2000, **113**, 9978– 9985.
12. E. Bitzek, P. Koskinen, F. Gähler, M. Moseler and P. Gumbsch, *Phys. Rev. Lett.*, 2006, **97**, 170201.